Materials Advances

ROYAL SOCIETY OF CHEMISTRY

PAPER

View Article Online
View Journal | View Issue

Cite this: *Mater. Adv.*, 2026, 7, 1495

Fabrication of a superabsorbent and pH-responsive glucomannan-based hydrogel: crosslinking, characterization, toxicological evaluation, and sustained-release of itopride

Fasiha Amjad,[a] Arshad Ali,[a] Muhammad Ajaz Hussain,[b]* Muhammad Tahir Haseeb,[c] Muhammad Farid-ul-Haq,[a] Izza Ajaz,[c] Muhammad Sher[a] and Muhammad Imran[d]

Herein, we describe the esterification of a polysaccharide-based hydrogel extracted from the sweet basil seeds using citric acid (CA). The formation of CA-crosslinked sweet basil seed hydrogel (CL-SBH) was ascertained through FTIR and solid-state CP/MAS ^{13}C NMR spectra. SEM analysis showed the existence of microscopic channels in CL-SBH. The CL-SBH was evaluated for its pH- and saline-dependent swelling properties. The highest swelling of CL-SBH was 17.83 g g^{-1} in DW and the lowest was 4.21 g g^{-1} at a pH of 1.2 after 480 min (8 h). During the swelling–deswelling studies, the CL-SBH displayed high swelling capacity in DW and in a buffer with a pH of 7.4, whereas the swelling was negligible in ethanol, normal saline, and in a buffer with a pH of 1.2 upon repeated cycles. Tablets based on CL-SBH and a drug (itopride) were prepared, and the results revealed that the itopride release was prolonged for 4 h at pH levels of 6.8 (97.75%) and 7.4 (94.63%), whereas approximately 36.75% of the drug was released at a pH of 1.2. The itopride release pattern followed first-order kinetics along with a Fickian diffusion mechanism. Acute oral and dermal toxicity studies of CL-SBH were conducted on Swiss albino rats and albino rabbits. The CL-SBH appeared non-toxic and non-irritating, as no change in hematological, biochemical, or histopathological parameters was observed in the animal models. Hence, the CL-SBH is a potential non-toxic material synthesized using a green crosslinking agent for prolonged, pH-dependent, and site-specific drug-delivery applications.

Received 6th September 2025,
Accepted 11th December 2025

DOI: 10.1039/d5ma01018g

rsc.li/materials-advances

1. Introduction

Polysaccharide-based hydrogels are superporous, superabsorbent, and stimuli-responsive biomaterials with considerably high swelling indices.[1–3] Polysaccharide-based hydrogels are used for biomedical applications because of their non-irritating, non-toxic, haemocompatible, non-immunogenic, economical, biocompatible, and biodegradable nature.[4,5] Additionally, polysaccharides exhibit highly diverse properties, *i.e.*, pH, temperature, salt-dependent swelling, stimuli-responsive swelling–deswelling, and sustained/intelligent drug delivery.[6] Polysaccharide materials show a wide range of utility in drug delivery, healthcare, food technology, water purification, and sustained-release drug-delivery systems.[7–11]

Seeds of *Ocimum basilicum* (sweet basil) excrete a gelatinous material upon immersion in deionized water (DW), which has been proven as a good source of edible gum and functional food, along with various applications in the pharma and health industries.[12–14] A study has indicated that the hydrogel from sweet basil mainly consists of glucomannan.[15]

In our previous reports on SBH, we use the native SBH[12,16] and its copolymeric derivative with methacrylic acid[17] to explore the stimuli-responsive swelling behavior of SBH in DW and at different pH levels (pH 1.2, 6.8, and 7.4), swelling–deswelling (on–off switching) properties *vs.* various stimuli, and acute oral toxicity studies. However, the present work will deal with the synthesis of CA-crosslinked SBH, *i.e.*, CL-SBH, in order to introduce a chemically modified network with a number of structural and functional advantages over the previously reported systems. The previously reported novel SBH-based hydrogel systems depend on physical entanglements and vinyl copolymerization. However, the hydroxyl (–OH) groups of

[a] *Institute of Chemistry, University of Sargodha, Sargodha 40100, Pakistan*
[b] *School of Chemistry, University of the Punjab, Lahore 54590, Pakistan. E-mail: majaz172@yahoo.com; Tel: +923468614959*
[c] *College of Pharmacy, University of Sargodha, Sargodha 40100, Pakistan*
[d] *Chemistry Department, Faculty of Science, King Khalid University, P.O. Box 9004, Abha 61413, Saudi Arabia*

SBH polysaccharides and the carboxyl (–COOH) groups of CA are connected through covalent ester cross-linking in the present CL-SBH hydrogel system. Structural integrity and resistance to early disintegration in aqueous or acidic environments may be greatly increased by this chemical modification. Moreover, the swelling and drug-release rates may be fine-tuned by carefully adjusting the ester crosslink density in the CL-SBH by varying the ratio of CA. Furthermore, CA provides an environmentally friendly substitute for synthetic cross-linkers like *N*,*N*′-methylenebisacrylamide, initiators, and hazardous solvents employed in previous research since CA is a non-toxic and biodegradable crosslinker. For oral and biomedical applications, CL-SBH will offer a more biocompatible and ecologically friendly solution. CA has been applied as a crosslinker for a number of naturally occurring hydrogels from seeds of *Mimosa pudica*,[18] *Cydonia oblonga*,[19] *Salvia spinosa*,[20] and *Aloe vera*.[21] CA is a biocompatible, stable in the gastric environment, and has no intrinsic pharmacological activity, such as prokinetic effects or D_2-receptor antagonism, thereby eliminating potential synergistic interactions with the drug under study. This ensures that any observed drug-loading behavior, gastric retention, or release kinetics can be attributed primarily to the material characteristics of the hydrogel.

Itopride (IP) hydrochloride is a benzamide derivative and prokinetic agent. IP has a short half-life (~6 h) and rapid absorption (T_{max}: 30–45 min), requiring multiple daily doses that cause fluctuating plasma levels and reduced patient compliance.[22–24] Because it is absorbed well in the upper GIT and is stable in gastric acid, a sustained-release formulation can therefore maintain therapeutic levels longer, reduce dosing frequency, and provide steadier prokinetic action. This improves symptom control, minimizes peak-related side effects, and enhances overall treatment efficiency.

Herein, we aimed to modify the swelling characteristics of glucomannan, a versatile polysaccharide isolated from the sweet basil seeds, by crosslinking it with CA to produce a smart and novel biomaterial CL-SBH for the controlled delivery of drugs, *e.g.*, IP. The goal was to characterize CL-SBH through FTIR, solid-state CP/MAS ^{13}C NMR, and SEM analyses to ascertain the crosslinking and morphology. The swelling behavior of CL-SBH was studied at different physiological pH levels. The swelling–deswelling attributes of CL-SBH were studied in DW *vs.* ethanol and normal saline and buffers of pH 7.4 *vs.* pH 1.2. Furthermore, CL-SBH is expected to achieve the sustained and site-specific release of IP across gastrointestinal pH ranges and exhibit no significant acute oral or dermal toxicity in animal models. This indicates its potential as a safe and effective drug-delivery system.

2. Materials and methods

2.1. Materials

Sweet basil seeds were purchased from a local market in District Sargodha, Pakistan. After the manual cleaning and removal of filthy materials, the seeds were stored in a vacuum desiccator. Analytical-grade potassium dihydrogen phosphate, *N*,*N*-dimethylacetamide (DMAc), 4-dimethylaminopyridine (DMAP), *n*-hexane, ethanol, NaCl, HCl, and KCl were procured from Riedel-de Haën (Germany). The base NaOH was standardized using oxalic acid, both of which were purchased from Merck, Germany. CA was purchased from Fischer Scientific, USA. DW was used throughout the study period. SBH was separated from the basil seed coats using nylon mesh. IP was used as a model drug and was of the United States Pharmacopeia standard.

2.2. Isolation of SBH

For the isolation of SBH (Fig. 1), an already reported procedure was adopted.[12] Briefly, cleaned basil seeds were immersed in DW (2 h), and extrudates were separated by rubbing the seeds between two layers of the nylon mesh. The SBH was washed with *n*-hexane and DW thrice to get rid of non-polar and polar impurities, respectively. The SBH was dried in a vacuum oven at 50 °C for 48 h, milled to obtain the fine powder, and stored.

2.3. Synthesis of CL-SBH

Dried and milled SBH (2 g) was added to DMAc (60 mL) and stirred at 100 °C for 2 h to achieve a homogeneous mixture. An aqueous solution of CA (5%, 100 mL) was added dropwise into the suspension of SBH. The catalyst DMAP (50 mg) was added, and the reaction proceeded for 24 h at 80 °C. The esterified product (CL-SBH-3), obtained after the precipitation of the reaction mixture in ethanol (200 mL), was washed in DW (100 mL). After drying and grinding, the CL-SBH-3 was stored. Three more CA-crosslinked derivatives of SBH were prepared using three different concentrations of CA, *i.e.*, 1.25% (CL-SBH-1), 2.5%

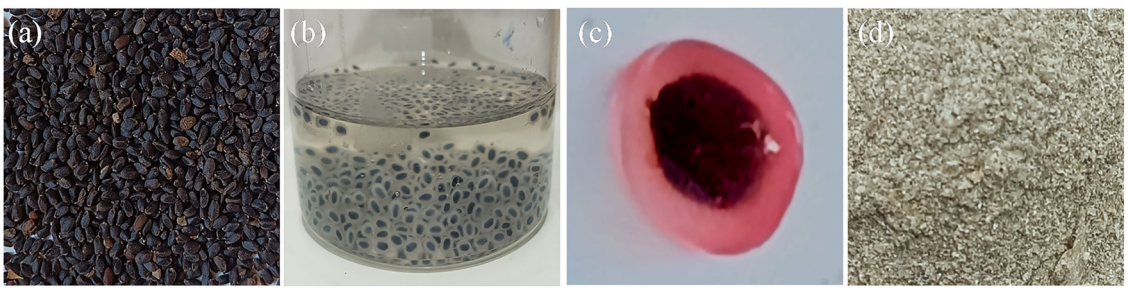

Fig. 1 SBH extraction scheme showing seeds of sweet basil in dry form (a), swollen seeds of sweet basil (b), swollen seed of sweet basil coated with the permitted red food color (c), and the SBH in dry form (d).

(CL-SBH-2), and 10.0% (CL-SBH-4) following the aforementioned procedure.

Yield: 74% (CL-SBH-1); 78% (CL-SBH-2); 82% (CL-SBH-3); 75% (CL-SBH-4).

Degree of substitution (DS) calculated from titration: 1.32 (CL-SBH-1); 1.47 (CL-SBH-2); 1.82 (CL-SBH-3); 1.41 (CL-SBH-4).

FTIR (KBr), CL-SBH-1: 1726 (C═O ester), 1037 (C–O–C) and 3383 (OH) cm^{-1}.

FTIR (KBr), CL-SBH-2: 1728 (C═O ester), 1049 (C–O–C) and 3522 (OH) cm^{-1}.

FTIR (KBr), CL-SBH-3: 1736 (C═O ester), 1107 (C–O–C) and 3689 (OH) cm^{-1}.

FTIR (KBr), CL-SBH-4: 1729 (C ═O ester), 1045 (C–O–C) and 3453 (OH) cm^{-1}.

The swelling of CL-SBH (all derivatives) in DW was noted to optimize the best concentration of CA. It was observed that among the samples prepared using 1.25%, 2.5%, 5%, and 10% of CA, the CL-SBH sample prepared using 5% of CA, *i.e.*, CL-SBH-3, showed higher yield, DS, and swelling in DW. Therefore, the quantity of this sample was enhanced for use in all the experimental work reported here.

2.4. Degree of substitution of CL-SBH

The degree of substitution of citrate moieties onto the backbone of SBH was determined by an acidimetric titration method using an already reported procedure with little amendment.[25] CL-SBH-1–4 (100 mg each) was dissolved and agitated for 2 h in an aqueous solution of NaOH with a known molarity (0.02 M). To titrate against a 0.01 M HCl solution (100 mL), the filtrate of the solution was collected. Methyl orange indicator was used to track the progress of the titration process. The DS value was determined using the equations (eqn (1) and (2)) by noting the final volume of HCl at the end of the titration.

$$n_{CA} = V_{NaOH} \times M_{NaOH} - V_{HCL} \times M_{HCL}, \quad (1)$$

where V_{NaOH} is the volume of the NaOH solution that was titrated against the net volume of V_{HCL}. M_{NaHCO_3} and M_{HCL} are the molarities of HCl and NaOH, respectively.

$$DS = \frac{162.14 \times n_{CA}}{m_{CL\text{-}SBH} - 100 \times n_{CA}}, \quad (2)$$

where n_{CA} represents the total number of moles of free –COOH groups of CA, $m_{CL\text{-}SBH}$ is the mass of relevant CL-SBH used to perform the titration, 100 is the increment additional to the mass of an AGU in g mol^{-1} for each replaced citrate moiety, and 162.14 is the molar mass (g mol^{-1}) as per anhydroglucose repeating unit (taking it as representative sugar) of SBH (AGU) for each citrate moiety.

2.5. Characterization

The FTIR (KBr pellets) spectra of SBH, before and after cross-linking, were recorded on an IR Prestige-21 spectrophotometer (Shimadzu, Japan) after drying for 30 min at 60 °C. The solid-state NMR (CP/MAS ^{13}C NMR) spectra of SBH and CL-SBH-3 were recorded on an NMR spectrophotometer (Bruker DRX-400). The SEM equipment (FEI Nova, Nano SEM 450, 10 kV) was equipped with an Everhart-Thornley detector. CL-SBH-3 (100 g) was mixed in DW in a mixer, milled, and degassed (30 min). Cross-sections of the swollen then freeze-dried samples (CL-SBH-3) were taken using a sharp blade to observe the channeling/pattern upon swelling. The obtained cross-sections of the sample were smeared with silver paint on an aluminum stub, followed by gold sputtering using a sputter coater (Denton, desk V HP), and SEM images were captured to study the morphology of the CL-SBH-3.

2.6. Swelling studies

2.6.1. pH-responsive swelling studies. For the determination of the swelling behavior of CL-SBH-3 in DW and at pH levels of 1.2, 6.8, and 7.4, the tea bag method was used.[26] The sample CL-SBH-3 (100 mg), packed in a tea bag, was hung in a swelling medium taken in a beaker. The CL-SBH-3 containing tea bags was weighed after predetermined time intervals to determine the swelling capacity (g g^{-1}). The swelling studies of CL-SBH-3 in each swelling medium were conducted till equilibrium was achieved for 480 min. The swelling capacity was calculated using the following equation (eqn (3)). The whole study was repeated three times, and the average value of the swelling capacity was calculated.

$$\text{Swelling capacity } (\text{g g}^{-1}) = \frac{W_t - W_c - W_0}{W_0}, \quad (3)$$

where W_0 is the weight of the dry powdered CL-SBH-3, W_t is the weight of the tea bag with the swollen CL-SBH-3, and W_c is the weight of the wet tea bag.

2.6.2. Swelling kinetics. The swelling results of CL-SBH-3 obtained in all the swelling media were used to determine the rate of solvent/swelling media absorption and extent of swelling. Hence, the normalized degree of swelling (Q_t) and the normalized equilibrium degree of swelling (Q_e) were calculated through eqn (4) and (5), respectively.

$$Q_t = \frac{W_s - W_d}{W_d} = \frac{W_t}{W_d}, \quad (4)$$

$$Q_e = \frac{W_\infty - W_d}{W_d} = \frac{W_e}{W_d}, \quad (5)$$

where W_d is the mass of CL-SBH-3 after drying at time $t = 0$, and W_s is the mass of CL-SBH-3 after swelling plus a wet tea bag at time t. W_e is the mass of the swollen medium remaining in the CL-SBH-3 at time $t = \infty$. W_t is the weight of DW entrapped in the CL-SBH-3 from the swelling medium at time t. W_∞ is the weight of the wet tea bag at equilibrium containing the swollen CL-SBH-3 at time t_∞.

The second-order swelling kinetics of CL-SBH-3 were determined by incorporating the values of Q_e and Q_t in eqn (6);

$$\frac{t}{Q_t} = \frac{t}{Q_e} - \frac{1}{kQ_e^2}. \quad (6)$$

The plot of t/Q_t *vs.* t yields a straight line, where the slope equals $1/Q_e$, and the intercept equals $1/kQ_e^2$, indicating that the swelling process follows second-order kinetics.

2.6.3. Saline responsiveness swelling. The sample CL-SBH-3 was evaluated for its saline-responsive behavior over 24 h using NaCl and KCl solutions at concentrations of 0.1, 0.2, 0.3, 0.4, 0.5, 1.0, 1.5, and 2.0 M. Powdered CL-SBH-3 (100 mg) was taken in tea bags (16), and each bag was placed in the aforementioned aqueous salt solutions separately. The swelling capacity of CL-SBH-3 in each solution was determined using eqn (3). Each swelling experiment was performed in triplicate, and the reported values represent the average of the three measurements.

2.6.4. On–off switching properties. The swelling–deswelling (on–off switching) behavior of CL-SBH-3 was evaluated by placing 100 mg of the hydrogel in a tea bag and immersing it in 100 mL of a buffer with a pH of 7.4. The swelling was monitored for 1 h, with the tea bag weighed every 15 min to calculate the swelling capacity using eqn (3). After 1 h, the swollen hydrogel was transferred into 100 mL of a buffer with a pH of 1.2 to assess deswelling. During this process, the swelling capacity was recorded at 15-min intervals using the same equation. This cycle of on–off switching was repeated four times; the cycle sets were repeated three times, and the mean values were recorded. The on–off switching properties of CL-SBH-3 in DW-ethanol and DW-normal saline was also conducted using the same method.

2.7. Drug release studies

2.7.1. Tablet preparation. IP was used as a model to evaluate the controlled-release potential of CL-SBH-3 for oral drug delivery. IP-loaded tablets (IPF) were prepared *via* the wet granulation method.[27] CL-SBH-3 (275 mg) and IP (150 mg, equivalent to a 50-mg TID daily dose) were thoroughly mixed using a mortar and pestle and then granulated using 5% w/v polyvinylpyrrolidone (PVP, 25 mg/0.5 mL). The granules were dried in a vacuum oven at 50 °C, passed through a no. 20 sieve, and lubricated with magnesium stearate (50 mg). Finally, the granules were compressed into 500 mg tablets using a rotary press with a 9 mm flat punch, achieving a hardness of 7–8 kg cm^{-2}.

2.7.2. *In vitro* itopride-release studies. The *in vitro* release of IP from IPF was carried out for 6 h at a pH of 6.8 using the USP Dissolution Apparatus II of Pharma Test, Germany (50 rpm and 37 °C). At predetermined time intervals, 5 mL samples were withdrawn from the dissolution vessels, and the volume was replenished with a fresh buffer with a pH of 6.8. The samples were filtered through a 0.45-μm nylon filter, diluted if necessary, and their absorbance was measured at 258 nm using a UV-vis spectrophotometer (UV-1600, Shimadzu, Japan).

2.7.3. IP-release kinetics and mechanism. The drug release kinetics and mechanism from IPF were studied by fitting IP-release data to the first-order kinetic and power law through eqn (7) and (8), respectively.

$$\log Q = \log Q_0 - \left(\frac{K_1 t}{2.303}\right), \tag{7}$$

where Q_0 is the amount of IP already present in the IPF, Q is the amount of IP that has not yet been released from the IPF, K_1 is a rate constant for the first-order, and t is the time at which a representative sample was collected.[28]

$$\frac{M_t}{M_\infty} = k_p t^n. \tag{8}$$

Here, M_t/M_∞ is the amount of IP released at time t, k_p denotes the Korsmeyer–Peppas constant, and n denotes the diffusion exponent. According to Ritger and Peppas, Korsmeyer *et al.*, and Siepmann and Peppas, the values of n express the drug release mechanism, *i.e.*, the values less than 0.45 (Fickian diffusion), between 0.45 and 0.89 (non-Fickian diffusion), at 0.89 (case-II transport), and over 0.89 (super case-II transport).[29–31]

2.8. Toxicity studies

The acute oral toxicity of CL-SBH-3 was assessed using albino rabbits (mean weight: 1420 g ± 20%) and Swiss albino rats (mean weight: 165 g ± 20%). Every animal, regardless of gender, was obtained from the University of Sargodha's animal house in Sargodha, Pakistan. After a comprehensive examination, the animals were moved to the laboratory and split into four groups of five animals each, strictly following Good Lab Practices (GLP) throughout the testing. Every animal was kept in a clean, well-maintained cage with regulated light, humidity, and temperature of 12 h photoperiod, 40%, and 25 °C, respectively. All the animals had unrestricted access to food and water, and they were fed a typical laboratory diet. All procedures for the toxicity studies were carried out following the OECD (Organization for Economic Co-operation and Development) guidelines.[32] The study protocol was formally approved by the Institutional Animal Ethics Committee of the University of Lahore, Pakistan (Approval No. IREC-2018-76-M, May 17, 2018). As per OECD guidelines, an *in vivo* oral acute toxicity investigation was conducted on the rats and rabbits. A dose of 0.05, 0.3, and 2 g kg^{-1} of the body weight of the rats and rabbits in groups S1, S2, and S3, respectively, was administered to monitor single-dose toxicity, whereas the control group was left untreated. Before CL-SBH-3 was given, all the animals were kept on a 12 h fast. The animals received a single dose of CL-SBH-3 that was more than the amounts of excipients they would normally consume each day. After 1 h of CL-SBH-3 administration, food and water were made freely available to the animals. After the delivery of CL-SBH-3, the animals' general health, particularly their salivation, diarrhea, tremors, and allergy symptoms, was monitored for 6 h. After the dose was administered, these parameters were monitored every day for 14 days.

The body weights of the rats and rabbits in the control group were recorded. The body weights of both animal species were recorded on the 1st, 2nd, 3rd, 7th, and 14th day after the administration of CL-SBH-3. The mean body weight of each group was calculated, and the difference between the animals of the treated and control groups was determined. The harmful effect of CL-SBH-3 on the overall health of the animals was determined by comparing the weights and food intake of the control and treated animals.

For the first three days, as well as on the 7th, 10th, and 14th days following that, the amount of food and water that the rats and rabbits in the control and treated groups consumed was tracked and recorded. To determine the impact of CL-SBH-3 on the animals' water and food consumption, the mean values of the water and food intake in the treated and control groups were computed, and the results obtained from the treated group were compared with those from the control group.

Five white albino rabbits were taken for primary eye irritation testing. Lesion scoring was done according to the Draize scale.[33] For this purpose, well-ground and finely divided CL-SBH-3 (30 mg) was moistened with a sufficient amount of DW, and the obtained thick paste was injected into the conjunctival sac of the right eye of each rabbit (treated groups). The left eye of the rabbits of the treated group was left untreated and labeled as control. The upper and lower eyelids of the treated rabbit eyes were gently held closed for 5 min to reduce loss of the applied material. The eyes were then observed for 72 h for signs of irritation, including redness, swelling, and lacrimation. The severity of erythema and edema was scored according to the Draize scale, and the total score was averaged over the number of observations. The rabbits were chosen as model animals to assess the acute dermal toxicity of CL-SBH-3. For this assessment, the OECD 402 guidelines were followed.[34] Accurately weighed CL-SBH-3 (0.2 g) was suspended in 5 mL of DW while being constantly stirred to prepare a thick paste. This paste was applied to the rabbits' shaved skin of their back limb and covered with a sterile surgical gauze pad. The rabbit skin was further covered using Micropore TM adhesive tape (3-inch wide) to prevent displacement. The pads were carefully removed after a day, and any signs of redness or rashes were noted.

Blood samples were obtained from the animals of the treated/sample and control groups on the 15th day, just before necropsy. The animals hearts were punctured to take blood, and the jugular arteries of rabbits were used to draw blood, which was then put into EDTA-lined tubes. Chloroform was used to anesthetize the animals. The various biochemical parameters in the blood samples of the animals were examined. Blood plasma was separated by centrifuging the samples at 4000 rpm for 30 min. The plasma levels of urea, cholesterol, uric acid, creatinine, triglycerides, alanine aminotransferase (ALT), and aspartate aminotransferase (AST) were then measured. Animals from both species were sacrificed to collect vital organs, including the small intenstine, stomach, kidney, liver, spleen, heart, and lungs. A macroscopic examination was performed to detect any lesions, and the absolute weights of each organ were recorded and compared with those of the control group.

The vital organs were preserved in formalin (10%, v/v) following the determination of the absolute organ weights. Using a sharp surgical blade, tissues that were 4–5 μm thick were cut to be examined for the toxicological effects of CL-SBH-3 on the architecture of important organs. Hematoxylin-eosin dye staining was done, and slides were examined under a microscope to look at cellular architecture.

2.9. Statistical analysis

The tests regarding swelling, swelling–deswelling, and drug release behavior were conducted three times, and the standard deviation (SD) was reported. The standard deviation (SD) was used to express the data gathered from various parameters for the animals in the control and treated groups. Statistical analysis was performed using one-way analysis of variance (ANOVA) in GraphPad Prism software. Differences were considered statistically significant at $p < 0.05$.

3. Results and discussion

3.1. Synthesis of CL-SBH

The CL-SBH (*i.e.*, SBH-1–4) samples were synthesized by the esterification of SBH with CA (Fig. 2a). The CA is first distributed homogeneously throughout the SBH matrix as an aqueous solution. Upon heating at 80 °C for 24 h, the CA undergoes intramolecular dehydration and converts cyclic anhydride intermediates *in situ*; these reactive anhydrides then acylate the –OH groups of the SBH groups and lead to the formation of covalent ester crosslinks, *i.e.*, CL-SBH hydrogel systems. Furthermore, during the reaction, a second anhydride of CA after attachment onto a polymer is formed *in situ*, which further reacts with the hydroxyl of the polymer randomly to generate CL-SBH.

3.2. Spectroscopic characterization

3.2.1. FTIR analysis. The FTIR spectra of SBH and CL-SBH-1–4 are shown in Fig. 3. The signals for OH, CH, C═O, and COC stretching absorption are assigned in the spectra. The formation of esters after the crosslinking of SBH with CA showed signals at 1712, 1728, 1736, and 1723 cm^{-1} for CL-SBH-1, CL-SBH-2, CL-SBH-3, and CL-SBH-4, respectively, indicating the success of the reaction.[20] The equilibrium swelling of all the derivatives of CL-SBH, *i.e.*, CL-SBH-1, CL-SBH-2, CL-SBH-3, and CL-SBH-4, was studied in DW for 12 h and found to be 18.50, 16.21, 14.11, and 13.78 g g^{-1}, respectively. Therefore, owing to the high swelling of CL-SBH-3 in DW, this derivative was upsized to conduct all the studies reported herein.

3.2.2. Solid-state CP/MAS ^{13}C NMR analysis. The solid-state CP/MAS ^{13}C NMR spectra of SBH before and after crosslinking with CA are shown in Fig. 4. The spectrum of SBH shows distinct sugar signals as broad peaks for anhydroglucose

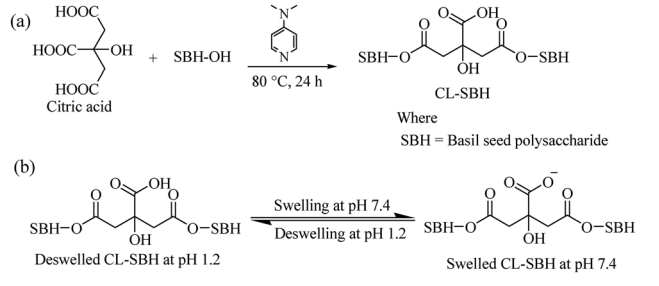

Fig. 2 Synthesis of CL-SBH using CA (a) and the swelling–deswelling mechanism of CL-SBH-3 at pH levels of 7.4 and 1.2 (b).

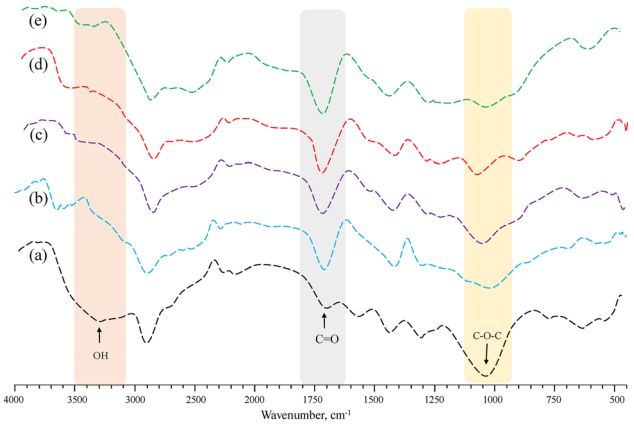

Fig. 3 FTIR spectra of the SBH (a), CL-SBH-1 (b), CL-SBH-2 (c), CL-SBH-3 (d), and CL-SBH-4 (e).

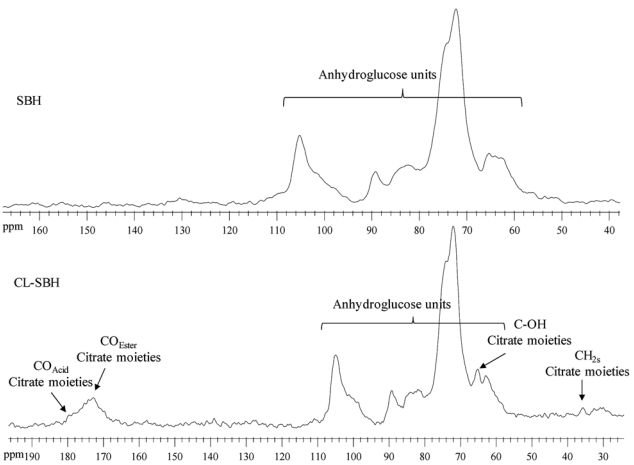

Fig. 4 Solid-state CP/MAS ^{13}C NMR spectra of the sweet basil seed hydrogel (SBH) before and after crosslinking (CL-SBH-3).

units or other sugars present in the sweet basil mucilage. The C1 and C6 of sugars appear at 105.47 and 63.21 ppm, respectively, whereas the C2–4 of sugars appears at 72.63–89.50 ppm. After chemical modifications, the crosslinked material, *i.e.*, CL-SBH-3, clearly indicated ester carbonyl signals at 172.92 ppm. In contrast, one unmodified COOH that remained free after conversion (see Fig. 4) appeared at 178.26 ppm, overlapping with esterified carbonyl groups. From the presence of distinct ester carbonyl absorptions in the FTIR spectra and the appearance of ester carbonyl signals in the solid-state CP/MAS ^{13}C NMR spectrum of CL-SBH-3, it is confirmed that SBH successfully crosslinked with CA.

3.2.3. SEM analysis. The findings of the SEM analysis are shown in Fig. 5 to get a better understanding of the topology of CL-SBH-3. The SEM images showed that CL-SBH-3 is porous and exhibits channeling. Owing to the pores, it can uptake a lot of DW and other physiological fluids.

3.3. Swelling studies of CL-SBH

3.3.1. pH-responsive swelling. The highest swelling index of CL-SBH-3 was observed in DW after 480 min, while at a pH of 1.2, negligible swelling was observed (Fig. 6a). The overall trend of swelling of CL-SBH-3 was observed as DW > pH 7.4 > pH 6.8 > pH 1.2. This is because, when CL-SBH-3 was added to the buffers with pH levels of 6.8 and 7.4, the –COOH groups present on its polymeric chain got ionized and resulted in the formation of anions. The resulting anions offered electrostatic repulsions between the corresponding anions. Consequently, the nearby polymeric chains were pulled apart by these anion–anion electrostatic repulsions, allowing the swelling media to enter the polymeric matrix. In response to this, the polymeric chains become loose and uncoiled, and the media easily penetrates them. As a result, the CL-SBH-3 swelling increased. Contrarily, the COOH groups on the polymeric chains of CL-SBH-3 remain un-ionized/protonated at an acidic pH of 1.2. As a result, CL-SBH-3 displayed insignificant swelling (off behaviour) at a pH of 1.2. A similar trend of pH-responsive

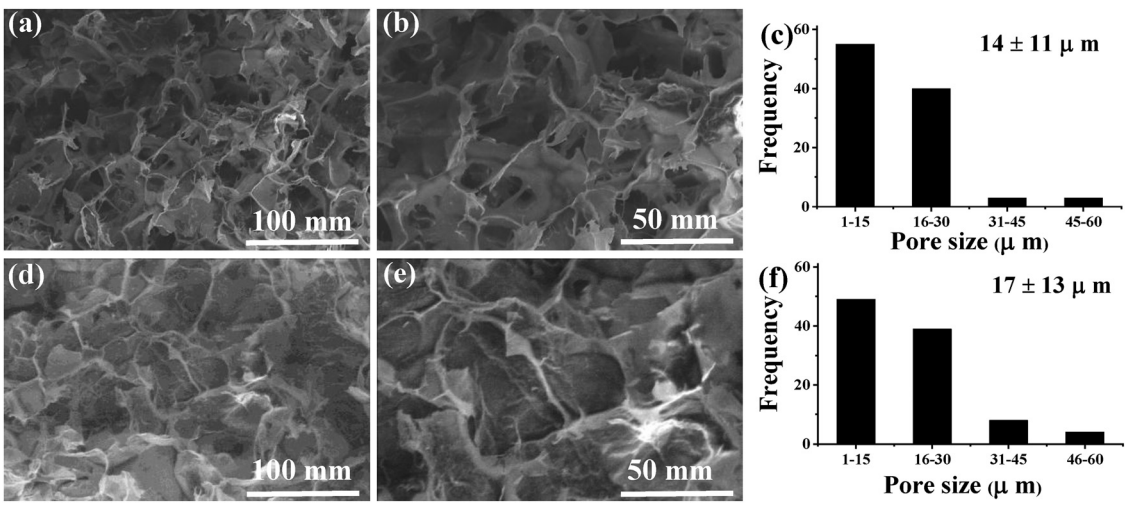

Fig. 5 SEM images of CL-SBH-3: transverse (a) and (b) and longitudinal (d) and (e). Histograms of CL-SBH-3: transverse (c) and longitudinal (f).

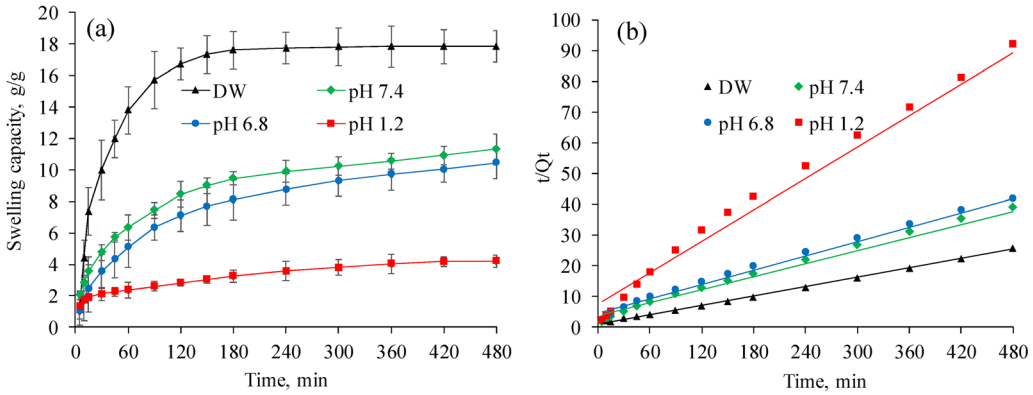

Fig. 6 Swelling (a) and swelling kinetics (b) of CL-SBH-3 at various pH levels.

swelling of structurally related biomaterials has been well documented.[18–21]

3.3.2. Swelling kinetics. The swelling profiles of CL-SBH-3 in DW and at pH levels of 7.4, 6.8, and 1.2 were analyzed to determine the swelling kinetics. The corresponding plots produced linear relationships, where the slope $1/Q_e$ and intercept $1/kQ_e^2$ were obtained with high correlation coefficients R^2. These results demonstrate that the swelling behavior of CL-SBH-3 is well described by a second-order kinetic model (Fig. 6b).

3.3.3. Saline responsive swelling. The swelling behavior of CL-SBH-3 was evaluated in NaCl and KCl solutions with varying molar concentrations. A progressive decrease in swelling was observed as the salt concentration increased from 0.1 to 0.5 M (Fig. 7a). This reduction is primarily attributed to the charge-screening effect, whereby elevated levels of Na^+ and K^+ ions diminish the electrostatic repulsion within the hydrogel network. Additionally, the rise in external salt concentration increases the osmotic pressure gradient between the hydrogel and the surrounding medium, further limiting water uptake and contributing to the reduced swelling. However, the swelling behavior of CL-SBH-3 remains constant when the salt contents in the solution are increased from 0.5 to 2.0 M.[35] CL-SBH-3 showed high swelling capacity in NaCl-based aqueous solutions

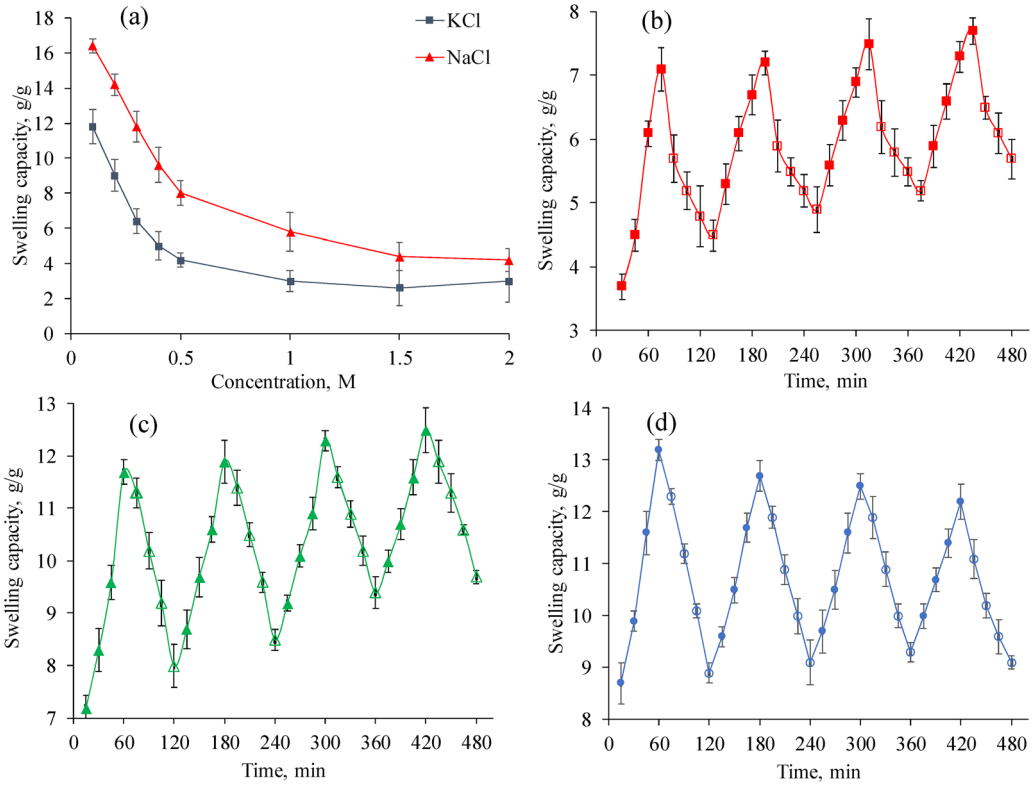

Fig. 7 Equilibrium swelling of the CL-SBH with varying NaCl and KCl concentrations (a); swelling–deswelling cycles at pH levels of 7.4 and 1.2 (b); in DW and normal saline (c); and in DW and ethanol (d).

of different molar concentrations as compared to KCl-based aqueous solutions of the same molar concentration. Both the Na^+ and K^+ ions carry the same uni-positive charge, *i.e.*, +1; however, the hydration radius of the Na^+ ion is greater than that of the K^+ ion, *i.e.*, 3.58 Å < 3.31 Å. Therefore, the Na^+ ion produced greater osmotic pressure than the K^+ ion and led to enhanced swelling. Moreover, owing to the large hydration radius and less charge density, Na^+ ions form weak electrostatic interactions with the negatively charged sites ($-COO^-$ groups) of the CL-SBH-3 hydrogel system. Such weak interactions between the Na^+ ions of NaCl-based solutions and $-COO^-$ groups of the CL-SBH-3 enhance the electrostatic attraction among the polymer chains and lead to an increase in the swelling of CL-SBH-3. Conversely, due to the smaller hydration radius, the K^+ ions form strong electrostatic interactions with the negatively charged sites ($-COO^-$ groups) of the CL-SBH-3 hydrogel system. Such strong interactions between the K^+ ions of KCl-based solutions and $-COO^-$ groups of the CL-SBH-3 reduce the electrostatic repulsion among polymer chains and lead to a suppression in the swelling of CL-SBH-3. Conclusively, due to the larger hydration radius and weaker binding to the $-COO^-$ groups of the Na^+ ion compared to those of the K^+ ion and weak polymer-ion interactions, the osmotic pressure will increase by reducing the charge screening effect, and the swelling of CL-SBH-3 in the NaCl solution increases.[36–38]

3.3.4. On–off switching properties

3.3.4.1. On–off switching properties at pH 7.4–1.2. The pH-responsive on–off switching properties of CL-SBH-3 were studied by dipping CL-SBH-3 (100 mg) in the swelling media (pH = 7.4) and then in deswelling media (pH = 1.2) after pre-determined time intervals. The CL-SBH-3 swelled rapidly in the swelling media, and upon shifting to the deswelling media, it deswelled abruptly and showed pH-responsive on–off switching behavior. The COOH of CL-SBH-3 was changed into its ionic form, COO-anion, at a pH of 7.4. The neighbouring polymeric chains repelled one another due to the electrostatic repulsion between these anions. Because of this, the swelling medium (buffer of a pH of 7.4) migrated within the polymeric matrix, causing CL-SBH-3 to rapidly swell.[18] When the pH was changed to 1.2, the swelling decreased because the COO-anion became protonated to COOH, hence CL-SBH-3 deswells.[20] After repeating the experiment for four successive cycles, similar findings were achieved, demonstrating its reproducibility (Fig. 7b). Furthermore, it was revealed that CL-SBH-3 did not show complete deswelling during the deswelling phase at a pH of 1.2 due to the presence of swelling media, *i.e.*, buffer of a pH of 7.4, trapped during the shifting to the deswelling media.

3.3.4.2. On–off switching properties in DW-normal saline. The on–off swelling behavior of the CL-SBH-3 was examined between DW and normal saline (Fig. 7c). CL-SBH-3 swelled significantly in DW but contracted in normal saline, primarily due to the charge-screening effect of Na^+ ions. The higher external ionic strength also reduces the osmotic pressure gradient, promoting water efflux from the hydrogel and leading to further shrinkage (Fig. 7b). After four consecutive cycles, CL-SBH-3 consistently exhibited its reversible saline-responsive behavior.

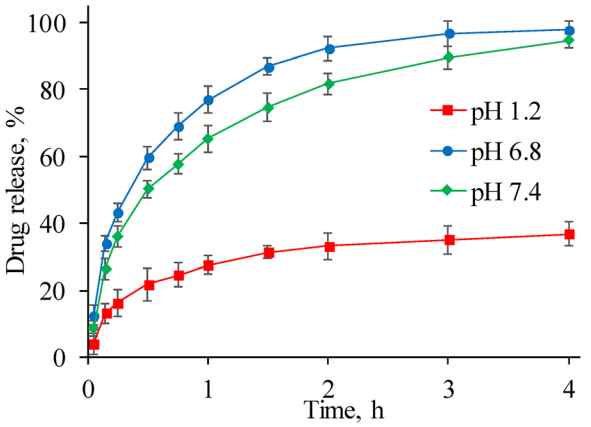

Fig. 8 Itopride release study from IPF at various pH levels of the GIT.

3.3.4.3. On–off switching properties in DW-ethanol. The on–off switching behavior of CL-SBH-3 was also studied in DW and ethanol. CL-SBH-3 showed high swelling in DW and deswelling in ethanol. The difference in the polarity and dielectric constant controls the on–off switching pattern in DW and ethanol, respectively. The CL-SBH-3 has polar groups in polymeric chains. Water is a polar solvent; hence, it forms hydrogen bonds with the polar groups of polymer chains. This way, water penetrates the matrix and chains are pushed apart, causing the swelling of the CL-SBH-3. However, ethanol is less hydrophilic and dehydrates the CL-SBH-3, making the chains to collapse, resulting in the shrinking of the CL-SBH-3 due to lower ionization. The on–off switching experiment was repeated four times and produced consistent results (Fig. 7d). In each cycle, CL-SBH-3 fully returned to its original deswelled state, confirming its stable and reversible ethanol-responsive behavior. These findings indicate that alcohol-containing beverages should be avoided when using a CL-SBH-3-based drug-delivery system, as ethanol may alter the release pattern and reduce therapeutic effectiveness.

3.4. Drug release studies

As CL-SBH-3 showed swelling at a pH of 1.2, the IP release experiments were performed at pH levels of 6.8 and 7.4. At a pH of 1.2, the incomplete IP release is due to the interaction of the drug-matrix combination as well as the pH-responsive swelling behaviour of the CL-SBH-3 hydrogel system. The CA cross-linking with SBH introduces –COOH groups into the CL-SBH, which causes the electrostatic repulsion inside the polymer chains of SBH to be suppressed at low pH levels, *i.e.*, a pH of 1.2. This is because these groups stay protonated (–COOH) instead of ionized ($-COO^-$). Consequently, the CL-SBH-3 network remains less swollen, more compact, and is responsible for limiting the drug (IP) from diffusing from the matrix and, finally, reduces water penetration. In acidic environments, such a decrease in the swelling of CL-SBH-3 and reduction of the

Table 1 Itopride release kinetics data

	First-order		Higuchi		Hixson–Crowell		Korsmeyer–Peppas		
	R^2	K_1	R^2	K_H	R^2	K_{HC}	R^2	K_{kp}	n
pH 6.8	0.9528	1.768	0.8575	67.530	0.8896	0.449	0.9521	71.471	0.356
pH 7.4	0.9175	1.151	0.9296	59.027	0.8440	0.316	0.9680	61.499	0.398

pore size is responsible for the insufficient release of IP at a pH of 1.2.[39] Another reason for the incomplete release of IP from CL-SBH-3 at a pH of 1.2 as compared to near neutral (pH = 6.8) and basic (pH = 7.4) conditions is the presence of strong hydrogen bonding between the polar groups, such as amine of methoxybenzamide portion of IP molecules, and protonated groups, such as –COOH and –OH of CL-SBH-3 at a pH of 1.2.[40] Contrast to the swelling behavior of CL-SBH-3, the IP release was more at a pH of 6.8 (97.75%) as compared with that at a pH of 7.4 (94.63%) because of the involvement of other parameters, *e.g.*, compression in the form of tablets, time of drug release, free mobility, and other physical dissolution conditions, *etc.* The release study of IP from IPF showed that CL-SBH-3 sustained IP release for up to 4 h and followed first-order kinetics under both pH conditions (Fig. 8 and Table 1). An analysis using the Korsmeyer–Peppas model indicated a Fickian diffusion mechanism, as the release exponent n was less than 0.45 at both pH levels.[31]

3.5. Toxicity studies of CL-SBH-3

3.5.1. Assessment of general conditions. During the 14-day toxicity study, the animals in the treated and control groups that received a single dose of CL-SBH-3 were found to be healthy and active. There were no signs of behavioral abnormalities, tremors, diarrhea, salivation, or lacrimation in any of the treated groups of rats or rabbits (Tables S1 and S2). Rats in Groups S1, S2, and S3 consumed somewhat less food on the first day after receiving CL-SBH-3, which may have been caused by their stomach feeling full. The LD50 value of the albino rats was found to be 6 g kg^{-1}; however, that of the rabbits was not established.

3.5.2. Assessment of body weight, food and water consumption. On days 1, 2, 3, 7, and 14, the body weight of the rats and rabbits of both groups was recorded. It was observed that the body weight of the animals in the sample groups was reduced on days 2, 3, and 5. After that, the weight gain of all the

Table 2 Hematological parameters and clinical biochemistry of rabbits

	Group C	Group S1	Group S2	Group S3
CBC				
TLC (μL^{-1})	8.6	7.6	9.2	7.3
RBC (μL^{-1})	6.2	5.2	5.7	6.6
Hb (g dL^{-1})	15.2	14.6	15.1	16.3
HCT (PCV) (%)	50.8	45.9	52.6	49.0
MCV (fL)	82.3	79.1	92.5	92.7
MCH (pg)	31.7	27.3	32.0	28.1
MCHC (g dL^{-1})	34.3	29.7	33.8	31.5
Platelet count (μL^{-1})	243.2	225.3	219.1	199.0
Neutrophils (%)	61.8	68.9	73.1	81.5
Lymphocytes (%)	28.1	32.4	24.1	38.9
Monocytes (%)	5.2	4.8	4.8	5.2
Eosinophils (%)	4.9	3.6	4.0	4.4
Lipid profile				
Cholesterol (mg dL^{-1})	173.5	158.8	181.2	178.4
Triglyceride (mg dL^{-1})	98.6	108.3	111.1	94.6
HDL (mg dL^{-1})	45.2	49.7	39.6	43.9
LDL (mg dL^{-1})	106.7	93.5	88.3	97.1
Liver function test				
Bilirubin (mg dL^{-1})	1.0	0.9	1.0	1.1
SGPT (ALT) (U L^{-1})	27.2	33.3	36.7	32.0
SGOT (AST) (U L^{-1})	23.2	20.8	21.6	23.7
ALP (U L^{-1})	29.4	33.1	32.5	29.3
Total protein (g dL^{-1})	7.4	6.6	7.8	6.2
Albumin (g dL^{-1})	4.3	4.1	3.9	3.4
Globulin (g dL^{-1})	3.5	3.7	3.3	3.4
Renal function test				
Urea (mg dL^{-1})	35.3	32.8	27.5	31.2
Creatinine (mg dL^{-1})	1.0	8.0	1.0	0.9
Hematology				
ESR (mm h^{-1})	9.3	9.5	8.2	9.2
Serum electrolyte				
Potassium (mmol L^{-1})	3.3	4.3	4.1	3.8
Sodium (mmol L^{-1})	141.6	138.2	145.9	151.2

Table 3 Hematological parameters and clinical biochemistry of rats

	Group C	Group S1	Group S2	Group S3
CBC				
TLC (μL^{-1})	6.3	6.4	5.8	5.3
RBC (μL^{-1})	5.8	5.1	4.9	5.5
Hb (g dL^{-1})	12.9	14.4	13.6	14.0
HCT (PCV) (%)	50.8	52.1	58.0	49.1
MCV (fL)	88.2	84.5	79.8	90.9
MCH (pg)	35.0	29.2	38.9	32.5
MCHC (g dL^{-1})	30.6	35.0	32.4	29.2
Platelet count (μL^{-1})	188.5	183.7	200.7	205.3
Neutrophils (%)	51.3	50.6	48.2	55.7
Lymphocytes (%)	23.8	27.9	28.4	25.8
Monocytes (%)	3.7	4.1	3.9	4.0
Eosinophils (%)	2.8	3.0	2.8	3.3
Lipid profile				
Cholesterol (mg dL^{-1})	127.4	136.9	131.8	128.6
Triglyceride (mg dL^{-1})	91.4	97.4	104.7	111.2
HDL (mg dL^{-1})	61.8	67.1	58.5	53.1
LDL (mg dL^{-1})	87.1	122.4	115.7	93.7
Liver function test				
Bilirubin (mg dL^{-1})	0.6	0.8	0.9	0.8
SGPT (ALT) (U L^{-1})	20.0	17.5	18.8	16.9
SGOT (AST) (U L^{-1})	14.8	16.9	22.3	18.0
ALP (U L^{-1})	21.5	19.2	20.8	18.9
Total protein (g dL^{-1})	7.4	7.6	8.2	8.5
Albumin (g dL^{-1})	4.3	43	3.7	4.1
Globulin (g dL^{-1})	3.9	4.1	3.3	3.8
Renal function test				
Urea (mg dL^{-1})	28.7	33.7	30.2	26.9
Creatinine (mg dL^{-1})	0.9	0.7	0.8	1.0
Hematology				
ESR (mm h^{-1})	5.6	6.7	6.3	5.4
Serum electrolyte				
Potassium (mmol L^{-1})	4.2	3.8	4.1	4.4
Sodium (mmol L^{-1})	146.9	123.5	139.3	141.1

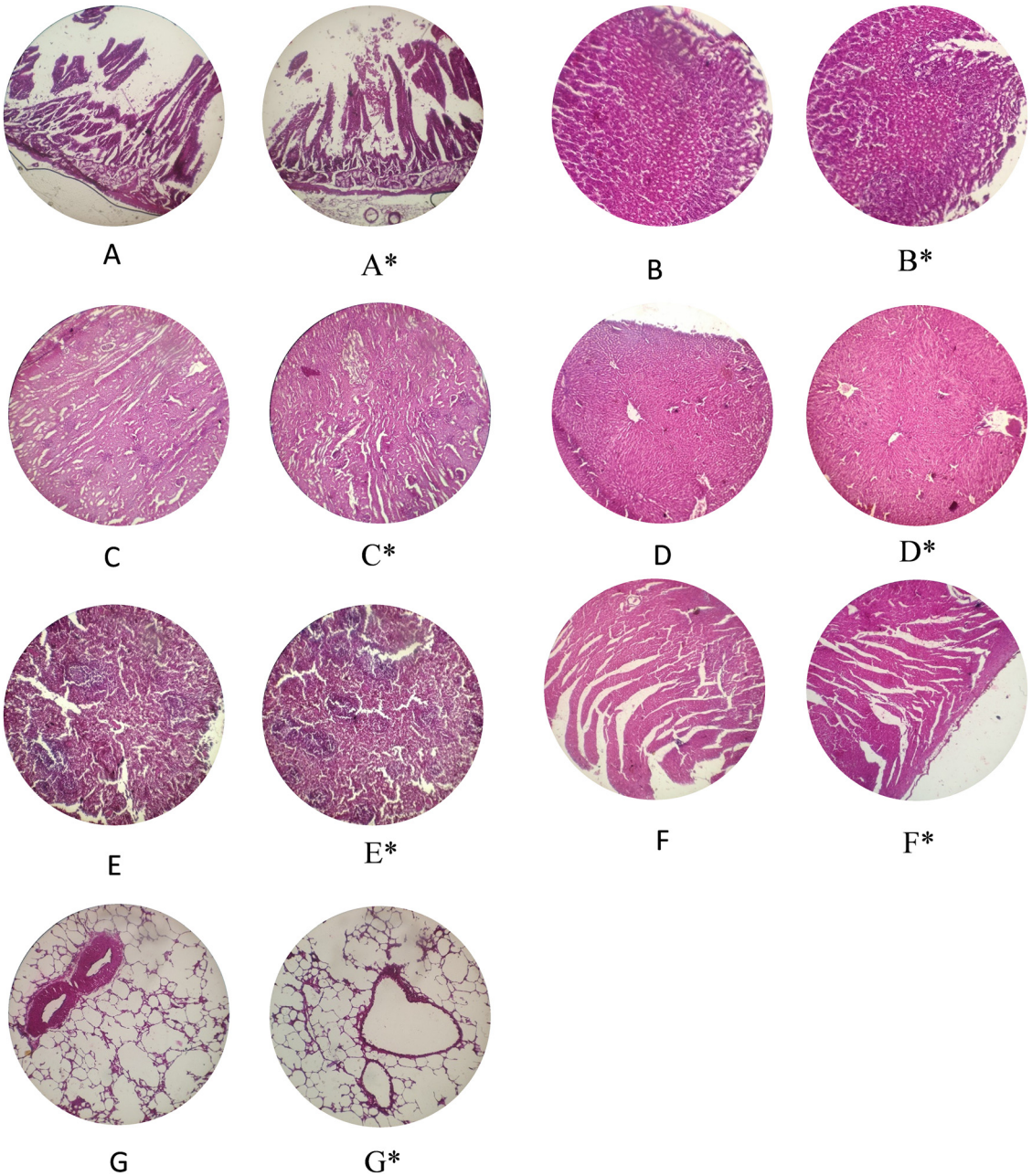

Fig. 9 Histopathology of the small intestine (A) and (A*); stomach (B) and (B*); kidney (C) and (C*); liver (D) and (D*); spleen (E) and (E*); heart (F) and (F*); and lungs (G) and (G*).

animals in the sample groups was observed. The weight loss could be associated with the reduced food intake, possibly due to the feeling of stomach fullness. During the second week of toxicity experiments, both the rats and rabbits in the treated groups displayed a normal rise in body weight comparable with the animals of the control group. The amount of food and water that the animals in the treated and control groups consumed was tracked every day on days 1–3. The amount of food and water that the rats and rabbits consumed on days 7–14 did not differ significantly from days 2–14. However, as the study progressed, the food and water consumption of the rats and rabbits in the sample was normalized and was comparable to that of the animals in the control (Tables S1 and S2).

3.5.3. Primary eye irritation testing. No signs of inflammation, irritation, conjunctivitis, or iritis were observed in any of the animals from the treated groups during the eye irritation test. All the animals in these groups were assigned a score of "0" according to the Draize scale. However, during the first 2 h of the animals from treated Group receiving CL-SBH-3, lacrimation was discovered in their right eye. These abnormalities subsided after 12 h and were statistically insignificant. Hence,

the abnormalities may be considered accidental and attributed to the mishandling and careless administration of CL-SBH-3.

3.5.4. Acute dermal toxicity. Following the conduction of acute cutaneous toxicity, the absence of lesion, abrasion, allergy, erythema, and infection symptoms suggests that CL-SBH-3 does not seem to be irritating and is considered a safe material for the development of dermal and transdermal drug-delivery systems.

3.5.5. Assessment of hematology and clinical biochemistry. The hematological markers, including RBCs, WBCs, and HBG, at normal levels show that CL-SBH-3 is safe. The hematological indicators in the treated and control groups did not significantly change during these studies (Tables 2 and 3). The normal outcomes of biochemical markers like lipid, liver, and renal profiles showed that CL-SBH-3 is a non-toxic drug-delivery vehicle. Normal ranges of the hematological parameters and clinical biochemistry of the rabbits and rats are shown in SI (see Tables S3 and S4).

3.5.6. Absolute organ body weight. On day 15, after sacrifice, the important organs of the rats and rabbits were excised, and their absolute weights were measured. No significant differences were observed in the organ weights between the treated and control groups (Tables S3 and S4).

3.5.7. Histopathology and gross necropsy. A histopathological examination of different organs in the rats following oral CL-SBH-3 treatment revealed no alterations in the cellular structure of the organs (*i.e.*, small intestine, stomach, kidney, liver, spleen, heart, and lungs). The absence of obvious signs of necrosis, hemorrhage, or inflammation would suggest that CL-SBH-3 is biocompatible for oral administration (Fig. 9).

4. Conclusion and future perspective

SBH was esterified with citric acid (CA) to prepare CL-SBH-3, a biocompatible hydrogel. The hydrogel exhibited remarkable stimuli-responsive swelling and reversible on–off switching properties, demonstrating its potential for use in oral formulations, particularly controlled-release tablets following first-order drug-delivery kinetics. CL-SBH-3 showed a high swelling capacity in distilled water (17.83 g g^{-1}) and in buffers at pH levels of 6.8 (11.3 g g^{-1}) and 7.4 (10.46 g g^{-1}), while the lowest swelling capacity was observed in a buffer at a pH of 1.2 (4.21 g g^{-1}). This behavior is advantageous for developing stomach-safe drug-delivery systems for non-steroidal anti-inflammatory drugs (NSAIDs), antibiotics, proton pump inhibitors (PPIs), and other acid-labile medications. The exceptional on–off switching properties of CL-SBH-3 allow the design of site-specific drug-delivery systems. These properties were demonstrated in swelling media, including DW and a buffer at a pH of 7.4, and in deswelling media, including a buffer with a pH of 1.2, normal saline, and ethanol. CL-SBH-3-based oral tablet formulations exhibited the highest release of IP at pH levels of 6.8 (97.75%) and 7.4 (94.63%), while the lowest release occurred at a pH of 1.2 (36.75%). Acute oral toxicity studies confirmed that CL-SBH-3 is non-toxic and non-irritating. This study demonstrates that CL-SBH-3 is a promising candidate for targeted and site-specific drug delivery to the intestine. Furthermore, its superporous and stimuli-responsive nature highlights its potential for use in a wide range of biomedical applications. Overall, CL-SBH-3 provides a foundation for the development of next-generation, safe, and pH-responsive materials for intelligent drug delivery, gastroretentive floating tablets, and other advanced biomedical applications.

Author contributions

Fasiha Amjad: investigation, writing – original draft. Arshad Ali: methodology, writing – original draft. Muhammad Ajaz Hussain: conceptualization, supervision, project administration, writing – review & editing. Muhammad Tahir Haseeb: validation, writing – review & editing. Muhammad Farid-ul-Haq: investigation, Izza Ajaz: formal analysis, writing – review & editing, Muhammad Sher: validation, resources. Muhammad Imran: formal analysis, resources.

Conflicts of interest

There are no conflicts to declare.

Data availability

No new data were generated or analyzed in the article.

Supplementary information (SI) is available. See DOI: https://doi.org/10.1039/d5ma01018g.

Acknowledgements

The authors express their appreciation to the Deanship of Scientific Research at King Khalid University, Saudi Arabia, for this work through the research group program under grant number RGP-2/528/46.

References

1 Z. Mirzakhanian, K. Faghihi, A. Barati and H. R. Momeni, Synthesis and characterization of fast-swelling porous superabsorbent hydrogel based on starch as a hemostatic agent, *J. Biomater. Sci., Polym. Ed.*, 2015, **26**, 1439–1451, DOI: 10.1080/09205063.2015.1100496.

2 M. Khatoon, A. Ali, M. A. Hussain, M. T. Haseeb, M. Sher, O. A. Alsaidan, G. Muhammad, S. Z. Hussain, I. Hussain and S. N. A. Bukhari, A superporous and pH-sensitive hydrogel from *Salvia hispanica* (chia) seeds: stimuli responsiveness, on–off switching, and pharmaceutical applications, *RSC Adv.*, 2024, **14**, 27764–27776, DOI: 10.1039/D4RA04770B.

3 M. A. Hussain, A. Ali, T. G. Alsahli, N. Khan, A. Sharif, M. T. Haseeb, O. A. Alsaidan, M. Tayyab and S. N. A. Bukhari, Polysaccharide-based hydrogel from seeds of *Artemisia vulgaris*: extraction optimization by Box–Behnken

design, pH-responsiveness, and sustained drug release, *Gels*, 2023, **9**, 525, DOI: 10.3390/gels9070525.

4 Y. Yang, L. Xu, J. Wang, Q. Meng, S. Zhong, Y. Gao and X. Cui, Recent advances in polysaccharide-based self-healing hydrogels for biomedical applications, *Carbohydr. Polym.*, 2022, **283**, 119161, DOI: 10.1016/j.carbpol.2022.119161.

5 A. Ali, M. A. Hussain, M. T. Haseeb, M. U. Ashraf, M. Farid-ul-Haq, T. Tabassum, G. Muhammad and A. Abbas, pH-responsive, hemocompatible, and non-toxic polysaccharide-based hydrogel from seeds of Salvia spinosa L. for sustained release of febuxostat, *J. Braz. Chem. Soc.*, 2023, **34**, 906–917, DOI: 10.21577/0103-5053.20230001.

6 N. Srivastava and A. R. Choudhury, Stimuli-responsive polysaccharide-based smart hydrogels and their emerging applications, *Ind. Eng. Chem. Res.*, 2023, **62**, 841–866, DOI: 10.1021/acs.iecr.2c02779.

7 H. Jing, X. Huang, X. Du, L. Mo, C. Ma and H. Wang, Anti-diabetic activity of a sulfated galactoarabinan with unique structural characteristics from *Cladophora oligoclada* (Chlorophyta), *Carbohydr. Polym.*, 2022, **278**, 118993, DOI: 10.1016/j.carbpol.2021.118933.

8 S. Y. Yao, M. L. Shen, S. J. Li, X. D. Wu, M. M. Zhang, L. N. Ma and Y. P. Li, Application of a mechanically responsive, inflammatory macrophage-targeted dual-sensitive hydrogel drug carrier for atherosclerosis, *Colloids Surf., B*, 2020, **186**, 110718, DOI: 10.1016/j.colsurfb.2019.110718.

9 J. S. Ribeiro, E. A. Bordini, J. A. Ferreira, L. Mei, N. Dubey, J. C. Fenno, E. Piva, R. G. Lund, A. Schwendeman and M. C. Bottino, Injectable MMP-responsive nanotube-modified gelatin hydrogel for dental infection ablation, *ACS Appl. Mater. Interfaces*, 2020, **12**, 16006–16017, DOI: 10.1021/acsami.9b22964.

10 M. A. Hussain, A. Abbas, M. G. Habib, A. Ali, M. Farid-ul-Haq, M. Hussain, Z. Shafiq and M. I. Irfan, Adsorptive removal of Ni(II) and Co(II) from aqueous solution using succinate-bonded polysaccharide isolated from *Artemisia vulgaris* seed mucilage, *Desalin. Water Treat.*, 2021, **231**, 182–195, DOI: 10.5004/dwt.2021.27468.

11 M. A. Hussain, A. Abbas, E. Yameen, A. Ali, G. Muhammad, M. Hussain and Z. Shafiq, Adsorptive removal of Pb^{2+} and Cu^{2+} from aqueous solution using an acid modified glucuronoxylan-based adsorbent, *Desalin. Water Treat.*, 2022, **248**, 163–175, DOI: 10.5004/dwt.2022.28088.

12 B. A. Lodhi, M. A. Hussain, M. Sher, M. T. Haseeb, M. U. Ashraf, S. Z. Hussain and S. N. A. Bukhari, Polysaccharide-based superporous, superabsorbent, and stimuli responsive hydrogel from sweet basil: a novel material for sustained drug release, *Adv. Polym. Technol.*, 2019, **2019**, 9583516, DOI: 10.1155/2019/9583516.

13 T. L. Western, The sticky tale of seed coat mucilages: production, genetics, and role in seed germination and dispersal, *Seed Sci. Res.*, 2012, **22**, 1–25, DOI: 10.1017/S0960258511000249.

14 H. C. Bravo, N. V. Cespedes, L. Zura-Bravo and L. A. Muñoz, Basil seeds as a novel food, source of nutrients and functional ingredients with beneficial properties: a review, *Foods*, 2021, **10**, 1467, DOI: 10.3390/foods10071467.

15 S. Nazir and I. A. Wani, Fractionation and characterization of mucilage from Basil (Ocimum basilicum L.) seed, *J. Appl. Res. Med. Aromat. Plants*, 2022, **31**, 100429, DOI: 10.1016/j.jarmap.2022.100429.

16 B. A. Lodhi, M. A. Hussain, M. U. Ashraf, M. Farid-Ul-Haq, M. T. Haseeb and T. Tabassum, Acute toxicity of a polysaccharide-based hydrogel from seeds of *Ocimum basilicum*, *Cell. Chem. Technol.*, 2020, **54**, 291–299, DOI: 10.35812/CelluloseChemTechnol.2020.54.31.

17 F. Amjad, A. Ali, M. A. Hussain, M. T. Haseeb, I. Ajaz, M. Farid-ul-Haq, S. Z. Hussain and I. Hussain, A super-absorbent and pH-responsive copolymer-hydrogel based on glucomannans from *Ocimum basilicum* (sweet basil): a smart and non-toxic material for intelligent drug delivery, *Int. J. Biolog. Macromol.*, 2025, **315**, 144452, DOI: 10.1016/j.ijbiomac.2025.144452.

18 M. A. Hussain, A. I. Rana, M. T. Haseeb, G. Muhammad and L. Kiran, Citric acid cross-linked glucuronoxylans: a pH-sensitive polysaccharide material for responsive swelling–deswelling vs various biomimetic stimuli and zero-order drug release, *J. Drug Delivery Sci. Technol.*, 2020, **55**, 101470, DOI: 10.1016/j.jddst.2019.101470.

19 M. A. Hussain, L. Kiran, M. T. Haseeb, I. Hussain and S. Z. Hussain, Citric acid crosslinking of mucilage from *Cydonia oblonga* engenders a superabsorbent, pH-sensitive and biocompatible polysaccharide offering on-off swelling and zero-order drug release, *J. Polym. Res.*, 2020, **27**, 49, DOI: 10.1007/s10965-020-2025-9.

20 A. Ali, M. A. Hussain, M. T. Haseeb, S. N. A. Bukhari, T. Tabassum, M. Farid-ul-Haq and F. A. Sheikh, A pH-responsive, biocompatible, and non-toxic citric acid cross-linked polysaccharide-based hydrogel from Salvia spinosa L. offering zero-order drug release, *J. Drug Delivery Sci. Technol.*, 2022, **69**, 103144, DOI: 10.1016/j.jddst.2022.103144.

21 J. Irfan, A. Ali, M. A. Hussain, M. T. Haseeb, M. Naeem-ul-Hassan and S. Z. Hussain, Citric acid cross-linking of a hydrogel from Aloe vera (*Aloe barbadensis* M.) engenders a pH-responsive, superporous, and smart material for drug delivery, *RSC Adv.*, 2024, **14**, 8018–8027, DOI: 10.1039/D4RA00095A.

22 S. M. Ahmed, A. Ahmed Ali, A. M. Ali and O. A. Hassan, Design and *in vitro/in vivo* evaluation of sustained-release floating tablets of itopride hydrochloride, *Drug Des., Dev. Ther.*, 2016, **10**, 4061–4071, DOI: 10.2147/DDDT.S115909.

23 Y. S. Kim, T. H. Kim, C. S. Choi, Y. W. Shon, S. W. Kim, G. S. Seo, Y. H. Nah, M. G. Choi and S. C. Choi, Effect of itopride, a new prokinetic, in patients with mild GERD: a pilot study, *World J. Gastroenterol.*, 2025, **11**, 4210, DOI: 10.3748/wjg.v11.i27.4210.

24 Y. Iwanaga, N. Miyashita, T. Saito, K. Morikawa and Z. Itoh, Gastroprokinetic effect of a new benzamide derivative itopride and its action mechanisms in conscious dogs, *Jpn. J. Pharmacol.*, 1996, **71**, 129–137, DOI: 10.1254/jjp.71.129.

25 A. Ali, A. Akram, A. B. Siddique, H. M. Amin, L. Zohra, A. Abbas, M. Sher, M. A. Hussain, M. T. Haseeb and M. Imran, A model batch and column study for Cd(II) uptake using citric acid cross-linked *Salvia spinosa* hydrogel: optimization through Box-Behnken design, *J. Ind. Eng. Chem.*, 2025, **151**, 746–761, DOI: 10.1016/j.jiec.2025.04.046.

26 M. T. Ban, N. Mahadin and K. J. Abd Karim, Synthesis of hydrogel from sugarcane bagasse extracted cellulose for swelling properties study, *Mater. Today Proc.*, 2022, **50**, 2567–2575, DOI: 10.1016/j.matpr.2021.08.342.

27 A. Khan, Prediction of quality attributes (mechanical strength, disintegration behavior and drug release) of tablets on the basis of characteristics of granules prepared by high shear wet granulation, *PLoS One*, 2021, **16**, e0261051, DOI: 10.1371/journal.pone.0261051.

28 M. Gibaldi and S. Feldman, Establishment of sink conditions in dissolution rate determinations: theoretical considerations and application to nondisintegrating dosage forms, *J. Pharm. Sci.*, 1967, **56**, 1238–1242, DOI: 10.1002/jps.2600561005.

29 P. L. Ritger and N. A. Peppas, A simple equation for description of solute release II. Fickian and anomalous release from swellable devices, *J. Controlled Release*, 1987, **5**, 37–42, DOI: 10.1016/0168-3659(87)90035-6.

30 J. Siepmann and N. A. Peppas, Modeling of drug release from delivery systems based on hydroxypropyl methylcellulose (HPMC), *Adv. Drug Delivery Rev.*, 2001, **48**, 139–157, DOI: 10.1016/j.addr.2012.09.028.

31 R. W. Korsmeyer, R. Gurny, E. Doelker, P. Buri and N. A. Peppas, Mechanisms of solute release from porous hydrophilic polymers, *Int. J. Pharm.*, 1983, **15**, 25–35, DOI: 10.1016/0378-5173(83)90064-9.

32 OECD, Guidelines for testing of chemicals: acute oral toxicity – Fixed dose procedure (No. 420), 2001, https://ntp.niehs.nih.gov/iccvam/suppdocs/feddocs/oecd/oecd_gl420.pdf.

33 J. H. Draize, G. Woodard and H. O. Calvery, Methods for the study of irritation and toxicity of substances applied topically to the skin and mucous membranes, *J. Pharmacol. Exp. Ther.*, 1944, **82**, 377–390.

34 OECD, Guidelines for testing of chemicals: acute dermal toxicity – Fixed dose procedure (No. 402), 2017, DOI: 10.1787/9789264070585-en.

35 C. Chang, M. He, J. Zhou and L. Zhang, Swelling behaviors of pH- and salt-responsive cellulose-based hydrogels, *Macromolecules*, 2011, **44**, 1642–1648, DOI: 10.1021/ma102801f.

36 O. Levy-Ontman, S. Nagar, O. Paz-Tal and A. Wolfson, Cation effect in polysaccharide-based hydrogel beads produced for europium adsorption from aqueous solutions, *J. Polym. Environ.*, 2024, **32**, 4017–4034, DOI: 10.1007/s10924-024-03196-7.

37 M. Mussel, P. J. Basser and F. Horkay, Ion-induced volume transition in gels and its role in biology, *Gels*, 2021, **7**, 20, DOI: 10.3390/gels7010020.

38 Y. Leng, C. N. Britten, F. Tarannum, K. Foley, C. Billings, Y. Liu and K. B. Walters, Stimuli-responsive phosphate hydrogel: a study on swelling behavior, mechanical properties, and application in expansion microscopy, *ACS Omega*, 2024, **9**, 37687–37701, DOI: 10.1021/acsomega.4c02475.

39 M. Suhail, Y. F. Shao, Q. L. Vu and P. C. Wu, Designing of pH-sensitive hydrogels for colon targeted drug delivery; characterization and in vitro evaluation, *Gels*, 2022, **8**, 155, DOI: 10.3390/gels8030155.

40 Y. Işıkver and D. Saraydın, Smart hydrogels: preparation, characterization, and determination of transition points of crosslinked N-isopropyl acrylamide/acrylamide/carboxylic acids polymers, *Gels*, 2021, **7**, 113, DOI: 10.3390/gels7030113.